Research Article / Araştırma Makalesi

3T MRI-Based Regional Mapping of Magnetization Transfer Ratio in Normal Brain Tissue: A Study of White and Grey Matter Differences

3 Tesla MRI Kullanılarak Normal Beyin Dokusunda Bölgesel Manyetizasyon Transfer Oranı Haritalaması: Beyaz ve Gri Madde Farklılıklarının İncelenmesi

Eyüp KAYA [1], Elif HOCAOĞLU [2], Ercan İNCİ [2], Veysel KAYA [1]
Mehmet TAHTABAŞI [3], Tanju KİSBET [4], Eyüp ÇAMURCUOĞLU [2]

[1]Department of Radiology, Faculty of Medicine, Harran University, Şanlıurfa, TÜRKİYE
[2]Heallth Sciences University, Bakırköy Dr. Sadi KONUK Training and Research Hospital, Department Of Radiology, Istanbul, TÜRKİYE
[3]Health Sciences University, Mehmet Akif İNAN Training and Research Hospital, Department Of Radiology, Şanlıurfa, TÜRKİYE
[4]Health Sciences University, Okmeydanı Training and Research Hospital, Department Of Radiology, Istanbul, TÜRKİYE

Abstract

Background: This study aimed to establish normal regional Magnetization Transfer Ratio (MTR) values in white and grey matter using 3-Tesla MRI in healthy adult subjects, with a particular focus on cortical and deep brain structures. It also aims to assess the variability of these values and provide a baseline for further pathological studies.
Materials and Methods: Seventy healthy volunteers (28 females, 42 males, mean age 28 years) were included. MRI scans were performed using a 3.0 Tesla MRI scanner. Conventional cranial MRI sequences were acquired, followed by Magnetization Transfer Imaging (MTI) with off-resonance pulses. MTR maps were generated from proton density-weighted images obtained with and without magnetization transfer pre-pulses. Measurements were performed in 31 white matter and 9 grey matter regions, with additional assessments of CSF for noise control. Statistical analysis was carried out to compare MTR values across different brain regions.
Results: The mean MTR value was significantly higher in white matter (23.9 ± 0.21) compared to grey matter (17.3 ± 0.77). The corpus callosum had the highest MTR values within the white matter, particularly in the splenium, while the thalamus exhibited the highest MTR values in the grey matter. Regional variations were observed, with higher MTR values in the occipital and temporal lobes and lower values in the frontal and parietal lobes. MTR measurements showed excellent intra-observer (ICC > 0.9) and good inter-observer reliability (ICC 0.80–0.90).
Conclusions: This study provides detailed MTR mapping of normal brain tissue, highlighting significant regional differences between white and grey matter. The findings offer valuable baseline data for assessing structural changes in CNS diseases and for evaluating the efficacy of therapeutic interventions. MTR measurements demonstrate high reproducibility, making this technique a reliable tool in clinical and research applications for monitoring pathological alterations in the central nervous system.

Keywords: Magnetization Transfer Ratio, MTR, 3.0 Tesla, Magnetization Transfer Imaging, brain.

Öz

Amaç: Bu çalışmanın amacı, sağlıklı yetişkin deneklerde 3 Tesla manyetik rezonans görüntüleme (MRG) kullanarak beyaz ve gri cevherde normal bölgesel Manyetizasyon Transfer Oranı (MTO) değerlerini, özellikle kortikal ve derin beyin yapılarına odaklanarak belirlemek, bu değerlerin değişkenliğini değerlendirmek ve daha ileri patolojik çalışmalar için bir temel oluşturmaktır.
Materyal ve metod: Çalışmaya dahil edilen 70 sağlıklı gönüllünün (28 kadın, 42 erkek, ortalama yaş 28) MRG taramaları 3.0 Tesla MRG tarayıcısı kullanılarak gerçekleştirildi. Konvansiyonel kranial MRG sekanslar elde edilmiş, ardından rezonans dışı darbelerle Manyetizasyon Transfer Görüntüleme yapıldı. MTR haritaları, manyetizasyon transferi ön darbeleriyle ve bunlar olmadan elde edilen proton yoğunluk ağırlıklı görüntülerden oluşturuldu. Ölçümler, gürültü kontrolü için ek BOS değerlendirmeleriyle birlikte 31 beyaz cevher ve 9 gri cevher bölgesinde gerçekleştirildi. Farklı beyin bölgelerindeki MTO değerlerini karşılaştırmak için istatistiksel analiz yapıldı.
Bulgular: Ortalama MTO değeri beyaz cevherde (23,9 ± 0,21) gri cevhere (17,3 ± 0,77) kıyasla önemli ölçüde daha yüksekti. Korpus kallozum, beyaz cevher içinde, özellikle spleniumda en yüksek MTO değerlerine sahipken, talamus gri cevherde en yüksek MTO değerleri saptandı. Oksipital ve temporal loblarda daha yüksek MTO değerleri ve frontal ve parietal loblarda daha düşük değerlerle bölgesel farklılıklar gözlendi. MTO ölçümleri mükemmel gözlemci içi (ICC > 0,9) ve gözlemciler arası iyi güvenilirlik (ICC 0,80–0,90) gösterdi.
Sonuç: Bu çalışma, normal beyin dokusunun ayrıntılı MTO haritalamasını sunarak beyaz ve gri cevher arasındaki önemli bölgesel farklılıkları vurgulamaktadır. Bulgular, MSS hastalıklarındaki yapısal değişiklikleri değerlendirmek ve terapötik müdahalelerin etkinliğini değerlendirmek için değerli temel veriler sunmaktadır. MTO ölçümleri yüksek tekrarlanabilirlik gösterir ve bu tekniği merkezi sinir sistemindeki patolojik değişiklikleri izlemek için klinik ve araştırma uygulamalarında güvenilir bir araç haline getirir.

Anahtar Kelimeler: Manyetizasyon Transfer Oranı, MTO, 3.0 Tesla, Manyetizasyon Transfer Görüntüleme, beyin.

Corresponding Author / Sorumlu Yazar

Dr. Mehmet Tahtabaşı
Health Sciences University, Mehmet Akif İNAN Training and Research Hospital, Department of Radiology, Şanlıurfa, TÜRKİYE

E-mail: mehmet.tahtabasi@sbu.edu.tr

Received / Geliş tarihi: 03.05.2025

Accepted / Kabul tarihi: 25.06.2025

DOI: 10.35440/hutfd. 1689766

This study was produced from a medical specialization thesis written in 2015. Thesis owner: Dr. Eyüp Kaya. Thesis number at the national thesis center: 10717915

Introduction

Magnetic resonance imaging (MRI) is a radiological tool which offers a sensitive, safe, and non-invasive way of imaging for central nervous system (CNS) diseases and monitoring the pathological alterations (1). The composed contrast in conventional MRI sequences results from the proton density of free-water molecules, and different relaxation characteristics of protons in water molecules. Thus, conventional MRI provides high sensitivity and low specificity for the detection of pathologies. Disease-related changes in water content or normal tissue losses due to edema, inflammation, infection, tumor cell infiltration, demyelinating diseases such as gliosis and other diseases which may cause neuronal damage can produce similar signal changes. Also, there is a proton pool which is tightly bounded to lipid membrane or proteins. Due to their very short T2 time, these protons are not visible in conventional MR images. Magnetization transfer imaging (MTI) is a MRI technique which can be used to collect indirect information about this bound proton pool and obtain information about a pathologic entity (1-3).

The pre-pulse method is used to selectively saturate the bound proton pool by using the resonance characteristics or differential T2 time of the free and bound protons. This saturation is transferred into free water protons in processes such as chemical transversion or spin diffusion, which result in significant decrease in the tissue signal intensity. Therefore, the size of this effect is known as the magnetization transfer ratio (MTR), which represents the quantity and nature of macromolecules in the areas of interest. It has been used increasingly to evaluate CNS-related diseases. In addition, it has a potential to investigate the efficacy of new experimental methods in multiple sclerosis (MS). The effects of variables such as age, sex, brain region, or dominant hemisphere on MTR values and other MTR-influencing variables should be known to interpret these studies accurately (4-13). In this study, we defined MTI method and referred clinical applications particularly in the field of neuroradiology. To serve a model for further pathological studies, we aimed to map regional MTR values in the normal white/grey matters (cortical-deep) in a group of adults using 3-Tesla MRI.

In light of these considerations, this study aims to explore the regional variations in Magnetization Transfer Ratio (MTR) values across different areas of the brain, particularly within the white and grey matter, using 3-Tesla MRI. By focusing on the normal cortical and deep regions in a cohort of healthy adults, we seek to establish baseline MTR values that can serve as reference points for future research into various CNS pathologies. This detailed mapping will help enhance the understanding of the relationship between tissue composition and MTR, further supporting its clinical applications in evaluating neurodegenerative and demyelinating diseases, such as multiple sclerosis.

Materials and Methods

Study Population

The study included a total of 70 volunteer healthy subjects without any pathology, as confirmed by conventional MRI. None of the subjects had any complaints. Before entering into the MRI room, all metal objects or accessories were removed. Exclusion criteria were as follows: having medical devices or equipment (internal fixation, metallic cover heart pacemakers, etc.) which can interfere with MRI imaging; age outside the pre-specified interval (range, 20 to 40 years); having measurement artifacts (confirmed by cerebrospinal fluid [CSF]); having a parenchymal pathology in conventional series, systemic disease, and chronic symptoms. The ethics committee approved the protocol of the study (Bakırköy Sadi Konuk Hospital, Ethics Committee, Number:2015/04/05). A written informed consent was obtained from each subject. The study was conducted in accordance with the principles of the Declaration of Helsinki.

MRI protocol

Images from all subjects were acquired in supine position with a 3.0 Tesla MRI Signal HD scanner (Siemens, MAGNETOM Verio, Germany) by using a head coil. Initially, the routine cranial MRI protocol was applied to all subjects; then, MTI sequencing was performed on subjects who fulfilled the inclusion criteria. For conventional images, preview images were acquired to determine the sections in the axial-sagittal and coronal planes. In accordance with the cranial MRI protocol, we obtained axial T1-weighted turbo spin echo (TSE) sequences, axial and coronal T2-weighted TSE sequences, axial fluid attenuated inversion recovery (FLAIR) sequences, and sagittal T1-weighted TSE sequence diffusion-weighted images and apparent diffusion coefficient (ADC) maps through this images.

Two different proton density-weighted images were obtained with/without using an off-resonance magnetization pre-pulse with the identical variables and the identical localization in the axial plane to create MTR map in the MTI. The following variables were used: TR: 2400 ms, TE: 18 ms, flip angle: 150˚, field of view (FOV) 220*180*180 mm, reconstruction matrix 128*128, voxel size: 1.88*1.88*3.00. Saturation pre-pulse was an off-resonance pulse with a frequency offset of 500 kHz and bandwidth of 488 Hz/px.

Images of 70 sections were used to screen the whole brain. Thirty-five sections were obtained by using the MTI pulse, and 35 sections were obtained without using the MTI pulse. After MRI, images were processed with MTR equation and, then, sent to workstations for analysis. The specific absorption rate (SAR) values were within the range of Food and Drug Administration-approved limits during measurements.

Image Analysis

All cross-sectional images were evaluated in syngo Acquisition Workplace-ICS Tower 11E by using the Syngo.via (Siemens Healthcare, Germany) software. The images were evaluated by two independent radiologists with nine (E.K.) and eight (V.K.) years of neuroradiology experience. The readers who performed the measurements evaluated the images independently and separately. In addition, for intraobserver variability, the same measurements were performed by the readers a second time at one-month intervals. Interobserver variability was evaluated by averaging the measurements made by the readers at different times. First, conventional images were analyzed to confirm the absence of underlying pathologies. Then, to provide process standardization, a guide list and image maps of measuring range were created. The MTR maps and T1-weighted images were measured after synchronization. The areas of interest in the MTR maps in all subjects were analyzed and saved accordingly. Both hemispheres were measured individually, and midline structures were measured alone. The MTR values were measured in the right/left hemispheres, white matter/grey matters (cortical–deep), all localizations in the white matter and supra and infratentorial compartments of the grey matter. The regional differences and mean MTR values with standard deviation (SD) of measured areas were statistically analyzed. In addition, MTR values of CSF samples were measured to provide noise control, and subjects with high noise values (CSF value >3 pu) were excluded. A total of 80 measurements were obtained from each subject; nine areas from the grey matter (i.e., cerebellum, temporal lobe, parietal lobe, precentral gyrus, occipital lobe, frontal lobe, head of the caudate nucleus, globus pallidus, putamen and thalamus) and 29 areas from the white matter (i.e., pericallosal area, brachium pontis, tectum, tegmentum, optic tract, middle and lateral cerebellar peduncles, central white matter of frontal lobe, frontal lobe U-fibers (subcortical WM), parietal lobe central WM, parietal lobe subcortical WM, temporal lobe central WM, temporal lobe subcortical WM, optical radiation, occipital lobe central WM, occipital lobe subcortical WM, internal capsule; anterior and posterior crus and genus, external capsule, corpus callosum genu and splenium, centrum semiovale, corona radiata, parasagittal subcortical WM, periventricular WM, pons, and cerebellar WM) were taken bilaterally and three midline WM (i.e., anterior commissure, fornix and body of corpus callosum) were taken unilaterally. The measurements of one CSF and total 79 parenchymal areas were evaluated with circular regions of interest (ROIs). The selected ROIs were chosen to cover both cortical and deep regions commonly involved in neurodegenerative and demyelinating diseases. The ROIs were between 0.5 mm^2 and 25 mm^2 depending on the region. The subjects with high CSF values (> 3pu) were also excluded.

Statically Analysis

All statistical analyses were performed using SPSS version 20.0 (SPSS Inc., Chicago, IL, USA). Variables were classified as either categorical or continuous. Categorical variables were presented as counts and percentages (%), while continuous variables were expressed as mean ± standard deviation. The intraobserver and interobserver agreement for MTR values in normal brain tissue were assessed using the intra-class correlation coefficient (ICC). ICC values were interpreted as follows: <0.4, poor agreement; 0.4–0.75, moderate agreement; 0.75–0.9, good agreement; and >0.9, excellent agreement (14-16). For example, the intra-observer ICC for the splenium of the corpus callosum was 0.94, indicating excellent reliability. Statistically, a p-value of <0.05 was considered significant for all analyses.

Results

A total of 70 subjects were included in the study. Of these subjects, 28 (40%) were females, and 42 (60%) were males. The mean age was 28 years (range, 20 to 40 years). For male subjects, the mean age was 29 years and 26.5 years for males and females, respectively.

Parenchymal MTR values of 41 areas (31 white matter areas, nine grey matter areas, and CSF) were measured for all 70 subjects. Thirty-seven parenchymal measurements were evaluated bilaterally, and three midline measurements were evaluated unilaterally (80 measurements for each subject). The mean MTR value in the white matter was higher, compared to the grey matter. The mean pu values for the grey matter and white matter were 17.3±0.77 (SD) and 23.9±0.21 (SD), respectively. The MTR maps showed homogeneous and uniform suppressions in the white matter and grey matter. In the grey matter, the lowest MTR values were obtained from the cerebellum and frontal lobe, while the highest values were obtained from the thalamus and globus pallidus. In the white matter, the lowest MTR values were obtained from the tectum, optic tracts, fornix, and anterior commissure, while the highest values were obtained from the corpus callosum, posterior crus, and centrum semiovale. In the comparison of the lobes, the highest mean MTR value was detected in the occipital and temporal lobes for the grey matter, whereas the white matter MTR value of the temporal lobe was higher than the other lobes. The mean MTR value in the subcortical white matter was lower, compared to the central white matter. According to the classification of the values of the, lowest to highest values were obtained from the anterior crus, anterior genu, and posterior crus, respectively. Values for the corpus callosum were homogenous, while the highest parenchymal MTR values were obtained from the corpus callosum splenium, followed by the corpus callosum genu. In the brainstem, suppression of the tectum was higher, compared to the mesencephalon and tegmentum.

In addition, higher values were observed in the lateral crus cerebri, compared to the medial crus cerebri. The MTR values in pons and tegmentum values were similar, which also

showed similarities to the MTR values in the white matter cerebellum. The MTR values in caudate nucleus and putamen values were close, while MTR values in globus pallidus were slightly higher. However, MTR values in the thalamus were higher, compared to the aforementioned regions. Tables 1 and 2 present the measurements performed by two different radiologists at two separate time points for white matter, along with the ICC values indicating intra- and inter-observer reliability.

Similarly, Tables 3 and 4 display the measurements performed by the same radiologists at two different time points for gray matter, along with the corresponding ICC values for intra- and inter-observer reliability. And the figures show the parenchymal levels at which the measurements were made.

The images in figures 1, 2, 3, 4, 5 and 6 show measurements in different regions.

Table 1. Intra-observer reliability of measurements of magnetic transfer rates from white matter

Localisation	Magnetisation Transfer Ratio (Reader 1)			Magnetisation Transfer Ratio (Reader 2)		
	First measurement	Second measurement	*R%*	First measurement	Second measurement	*R%*
1. Corpus Callosum body	24.3±0.5	24.8±1.1	93.8	24.4±1.2	24.9±1.1	90.1
2. Pericorpus callosum WM	24.5±0.7	24.1±0.7	91.2	23.9±0.7	24.1±0.6	84.1
3. Brachium pontis	23.2±0.8	23.3±0.7	96.1	23.0±0.6	22.8±0.8	87.2
4. Tectum	21.7±0.6	22.0±1.0	93.2	22.2±0.9	22.1±1.0	86.3
5. Tegmentum	23.1±0.7	23.0±0.9	96.8	23.1±0.9	22.9±0.9	90.2
6. Optic tract	22.0±1.0	21.4±1.5	97.8	21.7±1.4	21.4±1.2	83.7
7. Cerebral pedincul medial	23.5±0.9	23.6±1.3	97.7	23.4±1.2	23.9±1.2	86.7
8. Cerebral pedincul lateral	24.2±0.8	24.3±1.3	98.2	24.1±1.2	24.3±1.2	87.9
9. Frontal lobe central	24.1±0.9	24.8±0.9	88.7	24.5±1.0	24.6±0.9	92.1
10. Frontal lobe subcortical	23.6±0.9	24.3±0.9	87.1	24.1±0.8	24.2±0.8	89.1
11. Parietal lobe central	24.5±1.1	25.2±1.0	89.2	24.8±1.2	24.8±0.9	96.7
12. Parietal lobe subcortical	24.3±0.5	24.5±0.8	97.8	24.3±0.9	24.2±0.9	94.1
13. Temporal lobe central	25.0±0.6	25.7±1.0	90.1	25.3±1.3	25.3±1.1	97.1
14. Temporal lobe subcortical	24.5±0.8	25.1±1.1	91.2	24.7±1.2	24.5±0.9	94.2
15. Optic radiations	24.7±0.7	25.1±0.9	93.1	24.8±1.1	24.8±1.2	97.1
16. Occipital lobe central	24.5±0.9	24.9±0.8	92.5	24.6±0.8	24.7±0.7	96.2
17. Occipital lobe subcortical	24.0±1.1	24.3±0.8	95.2	24.1±0.9	24.3±0.8	93.4
18. Internal Capsul anterior Crus	24.2±0.8	23.5±1.1	89.8	23.4±1.1	23.5±0.9	97.5
19. Internal Capsul genu	24.6±0.7	24.6±1.0	98.7	24.3±1.1	24.6±1.1	89.8
20. Internal Capsul posterior Crus	25.3±0.7	25.5±0.9	96.2	25.1±1.2	25.3±1.1	95.2
21. External Capsul	23.0±0,5	23.1±0.8	97.1	23.1±0.7	22.5±0.9	92.1
22. Corpus Callosum genu	25.9±0.8	26.0±0.9	93.1	25.5±1.3	26.1±0.8	92.8
23. Corpus Callosum splenium	26.1±0.8	26.5±1.0	94.0	26.1±1.2	26.5±1.1	96.1
24. Fornix	21.8±0.7	21.6±1.1	96.4	21.9±1.2	21.2±1.0	87.4
25. Centrum semiovale	25.1±0.4	24.9±0.7	95.1	24.6±0.9	24.8±0.9	89.1
26. Corona radiata	24.2±0.5	24.3±0.9	97.1	24.1±0.9	24.1±0.8	96.5
27. Parasagital subcortical WM	24.1±0.4	23.9±1.0	96.3	23.8±0.9	23.7±0.7	97.4
28. Periventricular WM	24.0±0.6	23.8±0.9	94.1	23.6±0.8	23.7±0.8	98.1
29. Anterior commissur	21.4±0.9	21.3±1.4	97.3	21.6±1.3	21.2±1.1	92.1
30. Pons	23.2±0.6	22.7±0.8	93.9	22.7±0.7	22.4±0.7	98.1
31. Cerebellum	23.2±0.6	22.7±0.8	94.2	22.6±0.7	22.4±0.8	96.0

%R Relative coefficient of reliability

Table 2. Inter-observer reliability of measurements of magnetic transfer rates from white matter

Localisation	Mangnetisation Transfer Ratio		
	Reader 1 average measurement	Reader 2 average measurement	*R%*
1. Corpus Callosum body	24.6±0.8	24.5±1.1	84.4
2. Pericorpus callosum WM	24.3±0.7	24.0±0.6	83.2
3. Brachium pontis	23.2±0.7	22.9±0.7	87.2
4. Tectum	21.9±0.8	22.1±1.0	86.1
5. Tegmentum	23.0±0.8	23.0±0.9	89.2
6. Optic tract	21.7±1.3	21.5±1.3	87.8
7. Cerebral pedincul medial	23.6±1.1	23.6±1.2	87.7
8. Cerebral pedincul lateral	24.3±1.1	24.2±1.2	88.2
9. Frontal lobe central	24.5±0.9	24.6±0.9	88.3
10. Frontal lobe subcortical	23.9±0.9	24.2±0.8	85.4
11. Parietal lobe central	24.8±1.0	24.7±0.9	84.7
12. Parietal lobe subcortical	24.4±0.7	24.2±0.9	87.8
13. Temporal lobe central	25.2±0.8	25.2±1.1	89.1
14. Temporal lobe subcortical	24.9±0.9	24.6±1.0	83.2
15. Optic radiations	24.9±0.8	24.7±1.2	87.1
16. Occipital lobe central	24.7±0.8	24.7±0.8	82.5
17. Occipital lobe subcortical	24.1±0.8	24.2±0.8	85.2
18. Internal Capsule anterior Crus	23.8±1.0	23.5±0.9	89.8
19. Internal Capsule genu	24.6±0.8	24.5±1.0	90.7
20. Internal Capsule posterior Crus	25.4±0.9	25.2±1.0	90.2
21. External Capsule	23.0±0.9	22.8±0.8	87.1
22. Corpus Callosum genu	26.0±0.9	25.8±0.8	83.1
23. Corpus Callosum splenium	26.3±0.9	26.3±1.1	94.3
24. Fornix	21.7±0.9	21.5±1.0	86.4
25. Centrum semiovale	25.0±0.5	24.7±0.9	82.1
26. Corona radiata	24.3±0.7	24.1±0.8	87.1
27. Parasagittal subcortical WM	24.0±0.8	23.7±0.8	86.3
28. Periventricular WM	23.9±0.9	23.7±0.7	89.1
29. Anterior commissur	21.3±1.3	21.3±1.2	90.3
30. Pons	22.9±0.8	22.5±0.8	82.9
31. Cerebellum	22.9±0.7	22.5±0.8	87.2

%R Relative coefficient of reliability

Table 3. Intra-observer reliability of measurements of magnetic transfer rates from gray matter

Localisation	Magnetisation Transfer Ratio (Reader 1)			Magnetisation Transfer Ratio (Reader 2)		
	First measure-ment	Second meas-urement	*R%*	First measure-ment	Second measure-ment	*R%*
Cerebellum	13.6±1.4	13.8±1.4	92.7	13.2±1.1	13.6±1.2	91.8
Temporal lobe	16.7±1.4	16.5±1.4	97.3	16.3±1.2	16.1±1.4	96.3
Parietal lobe	16.2±1.9	16.3±1.7	95.4	16.0±1.1	16.2±1.7	94.4
Occipital lobe	16.2±1.4	15.9±1.2	90.8	16.0±1.3	15.8±1.3	91.4
Frontal lobe	14.2±1.6	14.3±1.3	94.9	14.0±1.4	14.5±1.2	93.9
Caudate nucleus	18.7±1.1	18.8±1.0	94.5	18.6±1.3	18.9±1.1	93.5
Globus pallidus	19.6±1.4	19.5±1.1	90.4	19.4±1.6	19.4±1.2	91.8
Putamen	22.5±1.1	22.3±0.9	91.0	21.5±1.1	22.1±0.8	90.0
Thalamus	22.9±1.1	22.6±0.9	87.9	22.6±1.4	22.4±0.9	91.9

%R Relative coefficient of reliability

Table 4. Inter-observer reliability of measurements of magnetic transfer rates from gray matter

Localisation	Magnetisation Transfer Ratio		
	Reader 1 average measurement	Reader 2 average measurement	*R%*
Cerebellum	13.7±1.4	13.4±1.2	89.7
Temporal lobe	16.6±1.4	16.2±1.4	87.3
Parietal lobe	16.6±1.9	16.1±1.7	85.4
Occipital lobe	16.0±1.4	15.9±1.3	91.8
Frontal lobe	14.3±1.6	14.3±1.2	91.9
Caudate nucleus	18.7±1.1	18.7±1.1	92.5
Globus pallidus	19.5±1.4	19.4±1.4	90.5
Putamen	22.4±1.1	21.8±0.8	89.8
Thalamus	22.7±1.1	22.5±0.9	88.9

%R Relative coefficient of reliability

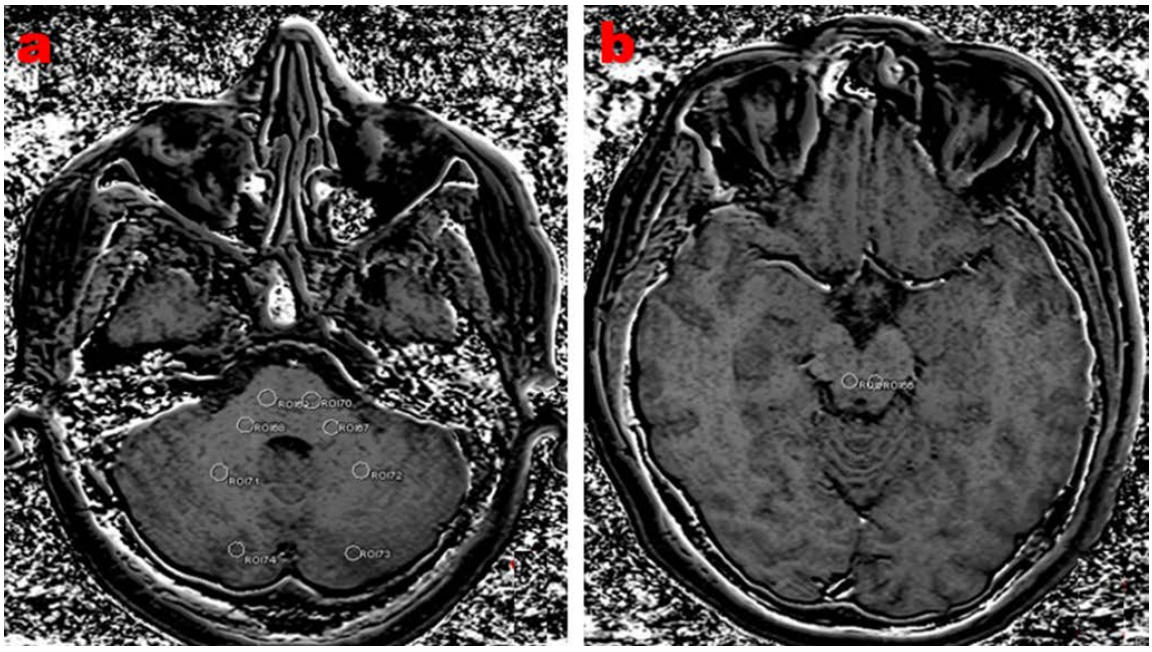

Figure 1. a) MTR measurement level from down to up. Pons level measurement examples: ROI 67-68: right and left middle, cerebellar pedincullus, ROI 69-70: Pons right and left half, ROI 71-72: right and left cerebellar white matter, ROI 73-74: right and left cerebellar gray matter **b)** inferior mesencephalic level. ROI 55-56: right and left Tegmentum

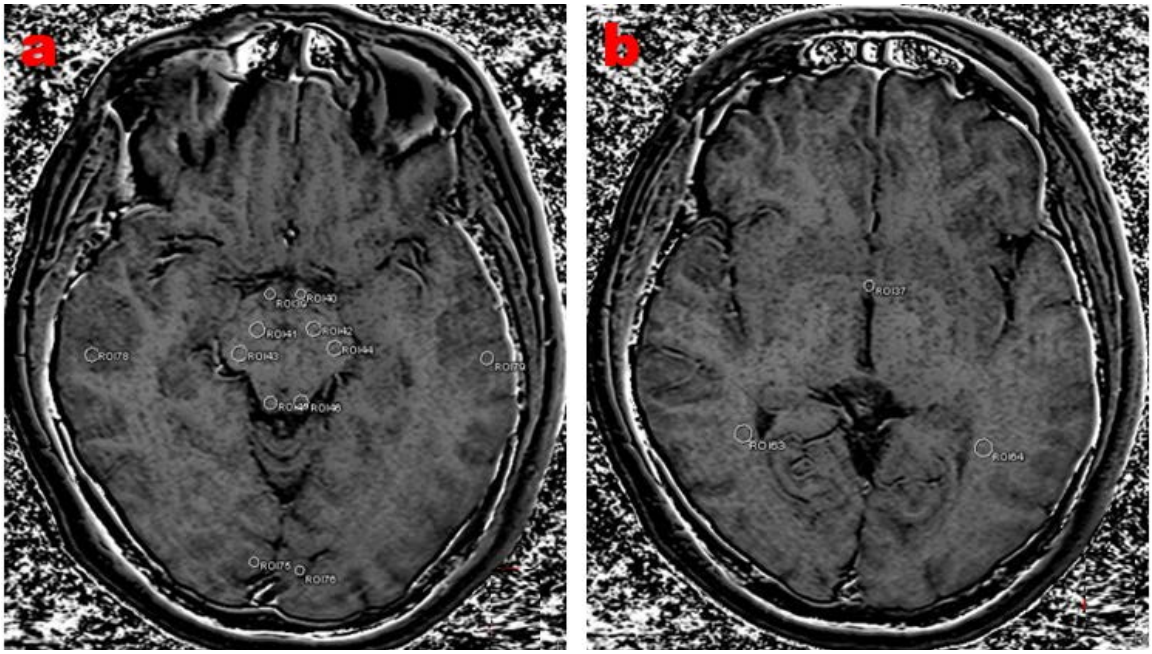

Figure 2. a) Superior mesencephalic level ROI 39-40: right and left optic tractus, ROI 41-42: right and left crus cerebri medial, ROI 43-44: right and left crus cerebri lateral, ROI 45-46 right and left half of tectum, ROI 75-76: right and left occipital gray matter, ROI 78 79: right and left temporal gray matter. **b)** Cerebrum basal level ROI 37: anterior commissur, ROI 63-64: right and left optic radiations

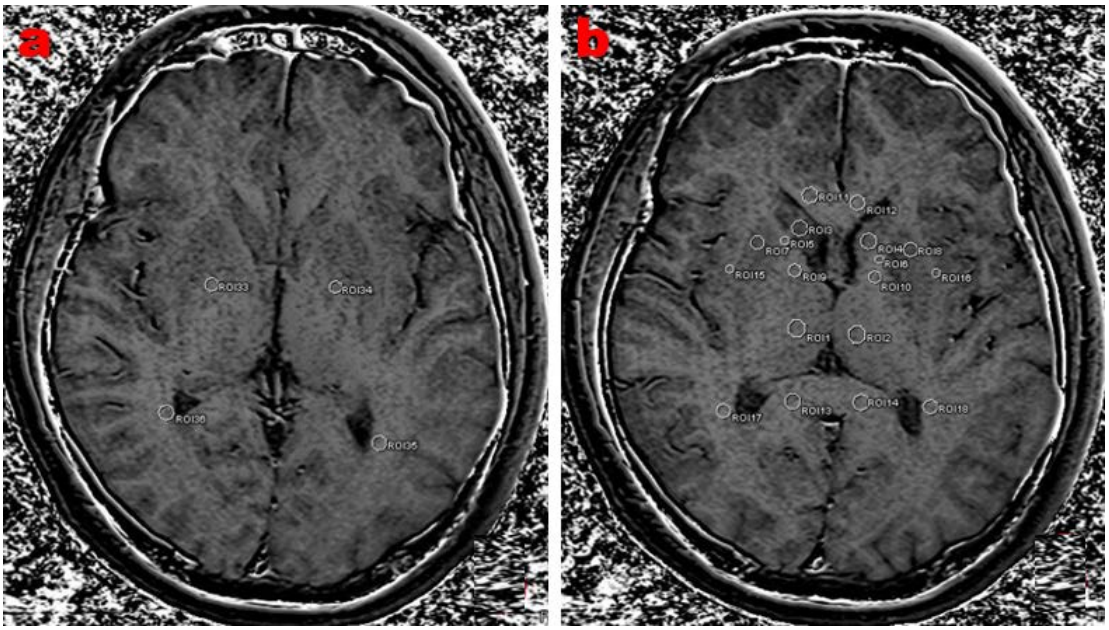

Figure 3. a) Inferior basal ganglia level. ROI 33-34: right and left globus pallidus, ROI 35-36: right and left periventricular white matter **b**) basal ganglia level
ROI 1-2: right and left thalamus ROI 3-4: right and left head of caudat nucleus
ROI 5-6: Right and left capsula interna anterior crus
ROI 7-8: Right and left putamen ROI 9-10: right and left capsula interna genu
ROI 11-12: Right and left halfs of corpus Callosum genu
ROI 13-14: Right and left halfs of Corpus Callosum splenium ROI 15-16: Right and left external capsule, ROI 17-18: Right and left periventricular white matter

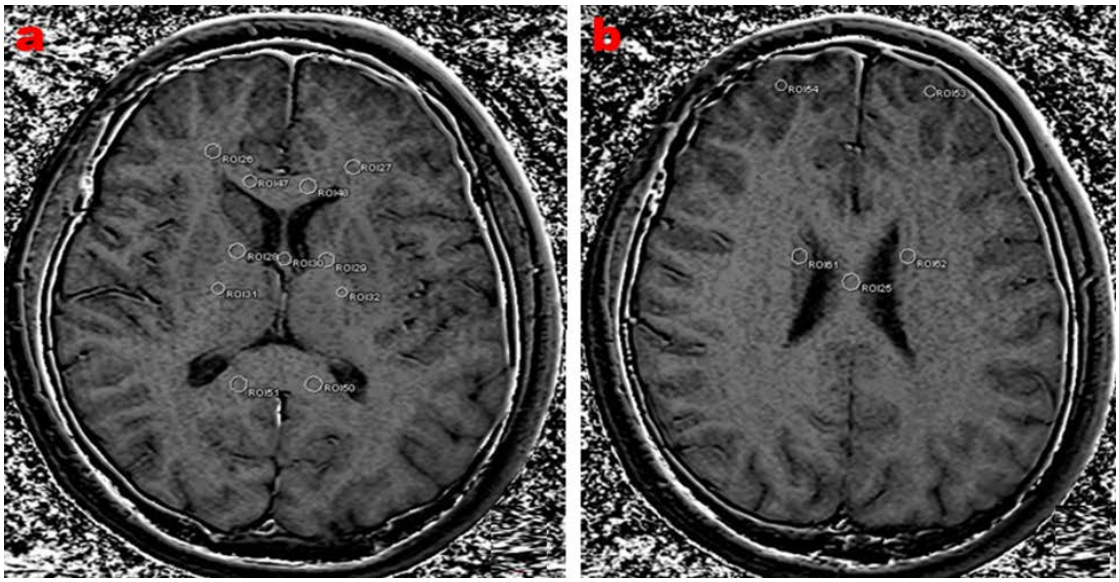

Figure 4. a) Upper basal ganglia level ROI 26-27: right and left pericorpus callosum
ROI 28-29: right and left internal capsule genu, ROI 30: Fornix, ROI 31-32: right and left internal capsule posterior krus ROI 47-48: Right and left halfs of Corpus Callosum genu
ROI 50-51: Right and left halfs of corpus callosum splenium. **b)** Upper ventriculary level. ROI 25: body of corpus callosum, ROI 51-52: right and left corona radiata, ROI 53-54: right and left frontal gray matter

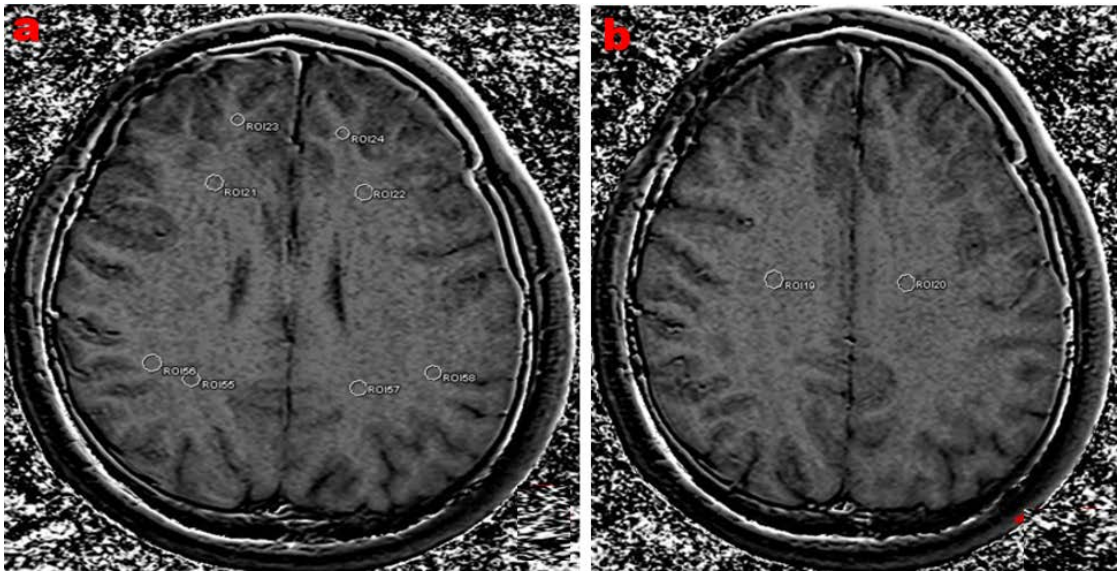

Figure 5. a) Supraventriculary level. ROI 21-22: right and left frontal deep white matter, ROI 23-24: right and left frontal subcortical white matter, ROI 55-57: right and left parietal deep white matter, ROI 56-58: right and left parietal subcortical white matter. **b)** upper centrum semiovale level. ROI 59-60: right and left parietal gray matter.

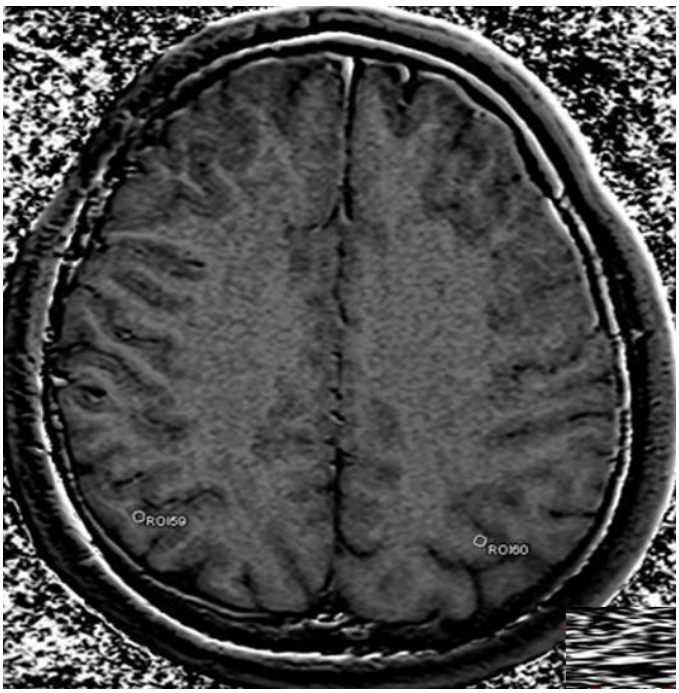

Figure 6. Centrum semiovale level. ROI 19-20: right and left centrum semiovale

Discussion

Tissue-contrast mechanisms in conventional MRI depend on three major features: density of free water protons, spin-lattice (T1), and spin-spin (T2) relaxations. Indeed, conventional MRI has low specificity in terms of detecting pathological processes. On the contrary, MTI has a unique contrast mechanism, which allows monitoring the macromolecule bound protons, which are not visible in conventional MRI (4). The MTR values in the brain have shown promise in detecting the structural damages of the white matter, demyelinating pathologies, particularly in disease such as MS (5,6,12,13). Regional MTR values and its variations of the normal brain should be known to understand how and what extent demyelinated white matter diseases alter the MTR values, which is considered more specific to structural white matter injury.

In this study, we identified regional MTR values in the normal white/grey matters (cortical-deep) in adults and evalu-

ated differences in the regional MTR values. We also discussed variations and possible reasons of these variations. We selected off-resonance MTI pulses with spin eco-based sequences to obtain MTR measurements. For dividing the brain into different zones, we used the table by Mehta et al. (17) with minor modifications, as it is helpful to evaluate more brain regions rather than other available methods (17,18).

Previous studies have demonstrated that MTR values vary among anatomic structures in the normal brain (1,17,18). The MTR values in the normal white matter are relatively high, compared to the grey matter (1,17,19). Moreover, MTR values show variations across different regions in the white matter; the highest MTR values are seen in the corpus callosum (1,17,20). The MTR value of the deep white matter is relatively low, compared to the corpus callosum. Different lobes have similar values. Subcortical U-fibers have lower MTR values. The highest MTR value in the grey matter is detected in the thalamus. Compared to thalamus, caudate nucleus, globus pallidum and putamen have similar, but relatively lower MTR values (17). Regional variations in myelination are accompanied by regional variations in MTR values. In addition, physiological age-related changes in MTR values have been observed in developing and adult brain (21,24). In another study, Engelbrecht et al. showed age-depended alterations in the MTR values in pediatric brain regions (22). The causes of the differential saturation are elevated myelination and galactocerebroside concentration due to the maturation (22). Mehta et al. (17) reported no significant differentiation between two-hemisphere, while Silver et al. (1) obtained higher values from left hemisphere. The differential MTR of the normal brain may be related to the fiber density, degree of myelination, degree of tissue hydration, and vascularization. The age-dependent and age-independent variations in MTR values in the normal brain should be considered in the analysis of regional MTR values in the affected brain.

In the present study, we used lower offset frequency (500 Hz) off-resonance pulse to decrease energy depolarization and as a result our MTR values were lower, compared to the previous findings. Our findings on the regional variations are consistent with findings of Mehta et al. (17) similar to previous studies; we observed higher MTR values in the white matter, compared to the grey matter (Tables 1,2,3 and 4-Figures 1, 2, 3, 4, 5 and 6). The degree of myelination, cerebroglycosides, phosphatidylcholine, and cholesterol in the white matter may have played a role in these results.

Moreover, we found the highest MTR values in the corpus callosum. Within the corpus callosum, the highest MTR value was detected in the splenium (Tables1 and 2-Figure 2). According to the literature data, corpus callosum has the highest MTR value within the white matter Within the carpus callosum, Mehta et al. (1) observed the highest MTR value in genu, while Silver et al. (1) and Garcia et al. (25) found the highest MTR value in the splenium. Corpus callosum has a large number (about 300 million fibers) of myelinated commissural fibers, which results in higher MTR values (26). Similar to Mehta et al. (17), we observed higher MTR values in the deep white matter, compared to the subcortical white matter at the lobar level (Tables 1 and 2-Figure 3).

Furthermore, the MTR values in the temporal and occipital lobes of the white matter were higher, compared to parietal and frontal lobes in our study (Tables 1 and 2-Figure 5). These results are also consistent with the findings of Mehta et al. (17). On the other hand, Silver et al. (1), Garcia et al. (25) and Tozer et al. (27) reported higher values in the frontal lobe. The MTR values in the periventricular white matter were similar, and MTR values in the centrum semiovale were higher, consistent with the literature (Tables 1and 2-Figures 2 and 3). In the internal capsule, as in the studies of Mehta et al. (17) and Garcia et al. (25), we observed the highest value in the anterior crus, followed by the anterior genu, and posterior genu (Tables 1 and 2-Figure 2). The MTR values in the posterior crus were higher, compared to the lobes of deep and superficial white matter (Tables1 and 2-Figures 2 and 3). Long and myelinated corticospinal tract fibers, which start from the primer motor cortex, constitute fibers of posterior crus, and the higher posterior crus values may be related to this.

In the evaluation of the structures of the posterior fossa white matter, we observed similar MTR values in pons, cerebellum, and brachium pontis, which were higher, compared to tectum and tegmentum. The lowest MTR values were observed in the tectum (Tables 1 and 2-Figure 1). There is no available data on MTR values in the pons and cerebellum in the literature. Mehta et al. (17) determined MTR values in tectum, tegmentum and brachium pontis. Contrary to our findings, the authors determined the highest MTR value in the tectum. Similar to Mehta et al. (17), we found higher MTR values in the lateral region of cerebral crus, compared to the medial region (Tables1 and 2-Figure 1). This can be due to the presence of fibers coming from posterior crus of internal capsule, whereas fibers coming from anterior crus of internal capsule and frontopontin fibers are present in the medial region.

Similar to the literature data, we determined the highest MTR value in the grey matter in the thalamus (Tables 3 and 4-Figure 2). A potential explanation for this finding is the presence of many afferent and efferent fibers in the thalamus (26). Consistent with the previous findings, we determined higher MTR values in the grey matter of the temporal lobe and the occipital lobe, which were lower compared to the basal ganglia (Tables 3 and 4-Figure 1).

In the comparison of the MTR values among basal ganglia, the highest value was found in the thalamus, followed by globus pallidus, putamen, and head of caudate nucleus (Tables 3 and 4-Figure 3). These findings are consistent with Garcia et al. (25); however, Mehta et al. (17) observed similar MTR values in the putamen and caudate nucleus, and higher MTR values, compared to the globus pallidus. Similar

to Garcia et al. (25), we found higher MTR values in the basal ganglia, compared to the other lobes. However, Mehta et al. (17) reported higher MTR values in the temporal lobe, compared to the globus pallidus.

Nonetheless, this study has a certain limitation as data were obtained from only a group of middle-aged individuals. Therefore, we were unable to evaluate the effect of age and dominance. However, we believe that our findings are highly valuable, as we used 3T-MRI to contribute to further studies.

In our study, we demonstrated that Magnetisation Transfer Ratio (MTR) measurements exhibit intra-observer agreement exceeding 90% (excellent agreement) and inter-observer agreement ranging between 80% and 90% (good agreement). These findings indicate that MTR measurements are highly reproducible and can yield reliable and accurate results even when performed by different observers. The results support the utility of MTR as a standardized measurement tool in both clinical practice and research settings.

Limitations

One limitation of this study is the relatively small sample size, which may affect the generalizability of the findings to the broader population. Additionally, while 3-Tesla MRI provides high-resolution imaging, the sensitivity of the MTR technique to detect subtle pathological changes in tissue composition may be limited by factors such as the resolution of the MRI scanner and the influence of motion artifacts. Furthermore, the cross-sectional design of the study prevents the assessment of longitudinal changes in MTR values over time, which could provide more insights into disease progression or the effects of treatment. Although hemispheric dominance was not assessed, previous studies have reported minimal impact of dominance on MTR values (28). Finally, other factors, such as individual variations in hydration status, medication use, or comorbidities, were not controlled for and could influence the MTR measurements.

Conclusion

In conclusion, MTR measurement has the potential to evaluate pathological and physiological structural alterations in CNS *in vivo*, and the method is an invaluable tool which can provide enhanced sensitivity and specificity in the evaluation of the pathological processes. In addition, MTR measurement has the potential to evaluate response to treatment, and therapeutic efficacy. On the other hand, biological variations in the normal brain regions should be considered in the interpretation of these findings. Therefore, we conclude normal MTR values in different brain regions to use as indices in further studies in which 3T MRI will be used with the variables described in this study.

Ethical Approval**:** *This study was approved by the Clinical Research Ethics Committee of the Bakırköy Sadi Konuk Training and Research Hospital (Ethical Committee approval number: 2015/04/05 Date: 23/02/2015).*

Author Contributions:
Concept: E.K.,V.K., M.T.,E.İ..
Literature Review: E.K., M.T., E.İ.
Design : E.K., M.T., T.K.
Data acquisition: M.T. E.Ç., T.K.
Analysis and interpretation: E.K., M.T.
Writing manuscript: E.K., M.T., V.K.
Critical revision of manuscript: E.K., M.T., T.K.

Conflict of Interest: *The authors have no conflicts of interest to declare.*

Financial Disclosure: *Authors declared no financial support.*

References

1. Silver NC, Barker GJ, MacManus DG, Tofts PS, Miller DH. Magnetisation transfer ratio of normal brain white matter: a normative database spanning four decades of life. J Neurol Neurosurg Psychiatry. 1997;62:223-228.
2. Van Gelderen P, Duyn JH. Background suppressed magnetization transfer MRI. Magn Reson Med. 2020;83(3):883-891.
3. Henkelman RM, Stanisz GJ, Graham SJ. Magnetization transfer in MRI: a review. NMR Biomed. 2001;14(2):57-64.
4. Wolff SD, Balaban RS. Magnetisation transfer contrast (MTC) and tissue water proton relaxation in vivo. Magn Reson Med. 1989;10:135-144.
5. Dousset V, Grossman RI, Ramer KN, Schnall MD, Young LH, Gonzalez-Scarano F, et al. Experimental allergic encephalomyelitis and multiple sclerosis: lesion characterisation with magnetization transfer imaging. Radiology. 1992;182:483-491.
6. Gass A, Barker GJ, Kidd D, Thorpe JW, MacManus D, Brennan A, et al. Correlation of magnetization transfer ratio with clinical disability in multiple sclerosis. Ann Neurol. 1994;36:62-67.
7. Tomiak MM, Rosenblum JD, Prager JM, Metz CE. Magnetization transfer: a potential method to determine the age of multiple sclerosis lesions. AJNR Am J Neuroradiol. 1994;15:1569-1574.
8. Hiehle JF, Grossman RI, Ramer KN, Gonzales-Scarano F, Cohen JA. Magnetization transfer effects in MR-detected multiple sclerosis lesions: comparison with gadolinium-enhanced spin-echo images and non-enhanced T1-weighted images. AJNR Am J Neuroradiol. 1995;16:69-77.
9. Ordidge RJ, Helpem JA, Knight RA, Quing Z, Welch KMA. Investigation of cerebral ischaemia using magnetization transfer (MTC) MR imaging. Magn Reson Imaging. 1991;9:895-902.
10. Dousset V, Armand JP, Degreze P, Mieze S, Lafon P, Caille JM. Progressive multifocal leucoencephalopathy studied by magnetization transfer imaging. In: Proceedings of the Society of Magnetic Resonance and the European Society for Magnetic Resonance in Medicine and Biology; 1995; Nice, France. p. 284.
11. Boorstein JM, Wong KT, Grossman RI, Bolinger L, McGowan JC. Metastatic lesions of the brain: imaging with magnetization transfer. Radiology. 1994;191:799-803.
12. Wong KT, Grossman RI, Boorstein JM, Lexa FJ, McGowan JC. Magnetization transfer imaging of periventricular hyperintense white matter in the elderly. AJNR Am J Neuroradiol. 1995;16:253-258.
13. Pirpamer L, Kincses B, Kincses ZT, Kiss C, Damulina A, Khalil M, et al. Periventricular magnetisation transfer abnormalities in early multiple sclerosis. Neuroimage Clin. 2022;34:103012.
14. Tahtabasi M, Kilicaslan N, Akin Y, Karaman E, Gezer M, Icen YK, et al. The Prognostic Value of Vertebral Bone Density on Chest CT in Hospitalized COVID-19 Patients. J Clin Densitom. 2021;24(4):506–515.
15. Kaya V, Tahtabasi M, Akin Y, Karaman E, Gezer M, Kilicaslan N. Prognostic Value of Vertebral Bone Density in the CT Scans of Sepsis Patients Admitted to the Intensive Care Unit. J Clin Densitom. 2023;26(3):101417.
16. Tahtabasi M, Erturk SM, Basak M. Comparison of MRI and 18F-FDG PET/CT in the Liver Metastases of Gastrointestinal and Pancreaticobiliary Tumors. Sisli Etfal Hastan Tip Bul. 2021;55(1):12-17.
17. Mehta RC, Pike GB, Enzmann DR. Magnetization transfer MR of the normal adult brain. AJNR Am J Neuroradiol. 1995;16:2085-2091.

18. Steens SC, van Buchem MA. MT: Magnetization Transfer. In: Quantitative MRI of the Brain: Measuring Changes Caused by Disease. John Wiley & Sons; 2003. p. 257-298.
19. Tofts PS, Sisodiya S, Barker GJ, Webb S, MacManus D, Fish D, Shorvon S. MR magnetization transfer measurements in temporal lobe epilepsy: a preliminary study. AJNR Am J Neuroradiol. 1995;16:1862-1863.
20. Hiehle JF Jr, Grossman RI, Ramer KN, Gonzalez-Scarano F, Cohen JA. Magnetization transfer effects in MR-detected multiple sclerosis lesions: comparison with gadolinium-enhanced spin-echo images and non-enhanced T1-weighted images. AJNR Am J Neuroradiol. 1995;16:69-77.
21. van Buchem MA, Steens SC, Vrooman HA, Zwinderman AH, McGowan JC, Rassek M, et al. Global estimation of myelination in the developing brain on the basis of magnetization transfer imaging: a preliminary study. AJNR Am J Neuroradiol. 2001;22:762-766.
22. Engelbrecht V, Rassek M, Preiss S, Wald C, Modder U. Age-dependent changes in magnetization transfer contrast of white matter in the pediatric brain. AJNR Am J Neuroradiol. 1998;19:1923-1929.
23. Steens SC, van Buchem MA. MT: Magnetization Transfer. In: Quantitative MRI of the Brain: Measuring Changes Caused by Disease. John Wiley & Sons; 2003. p. 257-298.
24. Berry I, Barker GJ, Barkhof F, Campi A, Dousset V, Franconi JM, et al. A multicenter measurement of magnetization transfer ratio in normal white matter. J Magn Reson Imaging. 1999;9:441-446.
25. Garcia M, Gloor M, Bieri O, Wetzel SG, Radue EW, Scheffler K. MTR variations in normal adult brain structures using balanced steady-state free precession. Neuroradiology. 2011;53:159-167.
26. Barr ML, Kieman JA. The human nervous system: an anatomical viewpoint. Philadelphia: JB Lippincott; 1993. p. 251-268.
27. Tozer D, Ramani A, Barker GJ, Davies GR, Miller DH, Tofts PS. Quantitative magnetization transfer mapping of bound protons in multiple sclerosis. Magn Reson Med. 2003;50(1):83-91.
28. Van Gelderen P, Duyn JH. Background suppressed magnetization transfer MRI. Magn Reson Med. 2020;83(3):883-891. doi:10.1002/mrm.27978.